

## Reconstruction of freeform surfaces for metrology

N El-Hayek<sup>1,4</sup>, H Nouira<sup>1</sup>, N Anwer<sup>2</sup>, M Damak<sup>3,4</sup> and O Gibaru<sup>4</sup>

<sup>1</sup> Laboratoire Commun de Métrologie (LNE-CNAM), Laboratoire National de Métrologie et d'Essais (LNE), 1 Rue Gaston Boissier, 75015 Paris, France,

<sup>2</sup> Ecole Normale Supérieure de Cachan, The University Research Laboratory in Automated Production, 61 avenue du Président Wilson, 94235 Cachan, France.

<sup>3</sup> GEOMNIA: 3D Metrology Engineering and Software Solutions, 165 Avenue de Bretagne, EuraTechnologies 59000 Lille, France,

<sup>4</sup> Arts et Métiers de Lille (ENSAM), Laboratory of information sciences and systems (LSIS), 8 Boulevard Louis XIV, 59046 Lille, France,

E-mail: [elhayek@lne.fr](mailto:elhayek@lne.fr)

**Abstract.** The application of freeform surfaces has increased since their complex shapes closely express a product's functional specifications and their machining is obtained with higher accuracy. In particular, optical surfaces exhibit enhanced performance especially when they take aspheric forms or more complex forms with multi-undulations. This study is mainly focused on the reconstruction of complex shapes such as freeform optical surfaces, and on the characterization of their form. The computer graphics community has proposed various algorithms for constructing a mesh based on the cloud of sample points. The mesh is a piecewise linear approximation of the surface and an interpolation of the point set. The mesh can further be processed for fitting parametric surfaces (Polyworks® or Geomagic®). The metrology community investigates direct fitting approaches. If the surface mathematical model is given, fitting is a straight forward task. Nonetheless, if the surface model is unknown, fitting is only possible through the association of polynomial Spline parametric surfaces. In this paper, a comparative study carried out on methods proposed by the computer graphics community will be presented to elucidate the advantages of these approaches. We stress the importance of the pre-processing phase as well as the significance of initial conditions. We further emphasize the importance of the meshing phase by stating that a proper mesh has two major advantages. First, it organizes the initially unstructured point set and it provides an insight of orientation, neighbourhood and curvature, and infers information on both its geometry and topology. Second, it conveys a better segmentation of the space, leading to a correct patching and association of parametric surfaces.

### 1. Introduction

Surface reconstruction is an inverse problem. It is the process of creating an approximation of a surface based on a cloud of points measured by optical and tactile probes. Many researchers worked on this subject and proposed a large number of solutions and scientific publications during the last 30 years. Delaunay and Voronoi-based meshing techniques [1] as well as implicit techniques [2] have been developed within the computer graphics community. These techniques relate to the problem of surface reconstruction where only the cloud of points is known and concern applications such as video games, arts and reverse engineering. Nonetheless, when studied closely and tested, these methods are ineffective unless two important initial conditions are fulfilled. The cloud of points must verify a



"good" sampling criterion and has to be free of noise [3]. The first Delaunay and Voronoi-based algorithms such as the sculpting algorithm of Boissonnat and the alpha shapes of Edelsbrunner and Mücke did not impose any of these conditions [4,5]. Hence, the resulting meshes were not strictly manifold. Amenta *et al* [6] presents proofs and guarantees for a "good" quality mesh reconstruction for the first time. Implicit techniques are based on a different philosophy and create an implicit representation of a surface. With the absence of model parameters, these approaches are not valid for metrology since no uncertainty budget can be established later on. Moreover, implicit surfaces techniques have no guarantees for surface reconstruction, meaning that no quality assessment can be done.

Freeform surfaces have seen enlarged applications since their complex shapes closely express a product's functional specifications and their machining is obtained with higher accuracy [7]. A freeform is a surface hardly defined by an equation or any generic form and is characterized by its asymmetric profile. According to ISO 17450-1 [8] freeform surfaces are complex geometrical features which have no invariance degree. However, these surfaces have proven their complex design functionalities [9]. This paper deals with datasets of an aspheric optical lens. The surface reconstruction algorithms tested on these datasets can have an extended usage on freeform surfaces. The datasets are measured at two metrology institutes by two different measurement strategies. LNE used a point-to-point measurement strategy on an XY grid. TNO (Netherlands Organisation for Applied Scientific Research) has measured the same optical lens on its high precision measuring machine Nanomefos with a spiral-like measurement strategy.

The 3D metrology of freeform surfaces is not yet normalized as no unified approach exists [10]. It differs from one application to another. Aspheric lenses inspection requires form characterization in some cases [11] [12] and simple profile characterization in some other cases. In form characterization the global surface is of interest. Whereas in profile characterization, only points along a cross-sectional plane at a specific location are considered. If not enough points can be found within the intersection of the cutting plane and the point set or if the level of the measurement noise is large, which is typically the case, surface reconstruction becomes mandatory. Either ways, form and/or dimensional characteristics are checked for conformity with respect to the design specifications.

This paper is focused on the study of meshes based on the Delaunay and Voronoi combinatorial structures. A mesh is a linear interpolation of the points that builds a structure on them. The initially unstructured point set becomes organized and structured. The mesh is a linear approximation of the underlying surface, which gives an insight of its topology and geometry. Discrete differential metrics can be calculated and used for further processing such as filtration, partition and association. Association is of various nature depending on the type of input provided with the cloud of points. If an analytical implicit model of the surface, such as the case of aspheric surfaces, is given, the association of that model to the structured points can be performed [11]. Whereas if no model is given, parametric models are fitted.

## 2. Delaunay and Voronoi structures

The Delaunay triangulation and Voronoi diagram are dual representations that infer complete knowledge about spatial neighbourhood. They build a structure that allows determining a point's exclusive neighbours. The Voronoi diagram is built based on this notion of proximity and cuts space into neighbourhood cells (3). Each point  $x$  in the space is assigned to one single point  $p$  in the dataset  $P$  as being in its exclusive neighbourhood. The Delaunay triangulation is a simplicial complex that connects the points that are exclusive neighbours among themselves. It is also known as a triangulation of the convex hull of the dataset. Triangulation is a broad word referring to tetrahedralization in 3D and triangulation in 2D, but we use it for simplicity. The simplices forming the 3D Delaunay complex are tetrahedra as opposed to triangles in two dimensional Delaunay complexes. Figure 1 shows how a Delaunay simplex is circumscribed in a circle empty of other points in the dataset. The general course of the surface reconstruction algorithms hereafter starts with the 3D Delaunay triangulation of the point set and then extracts a triangular surface mesh from it. Only

triangles that approximate the underlying surface are selected in the output mesh. These triangles constitute the set of restricted Delaunay simplices. The Delaunay triangulation grants the most regular triangulation, as it builds the most equiangular triangles possible [13]. The duality between Voronoi and Delaunay is done according to their simplices dimensions. By taking  $n=3$  as the dimension of the ambient space, a 0-simplex (vertex) of the Delaunay triangulation corresponds to a  $n$ -simplex (Voronoi cell) of the Voronoi diagram. Similarly, a 1-simplex (edge), 2-simplex (triangle) and  $n$ -simplex (tetrahedron) in the Delaunay triangulation, correspond to a  $(n-1)$ -simplex (Voronoi facet), a  $(n-2)$ -simplex (Voronoi edge) and a 0-simplex (Voronoi vertex) in the Voronoi diagram, respectively.

$$Vor(p) = \{x \in \mathbb{R}^d \mid d(x, p) \leq d(x, q), \forall q \in P\} \quad (1)$$

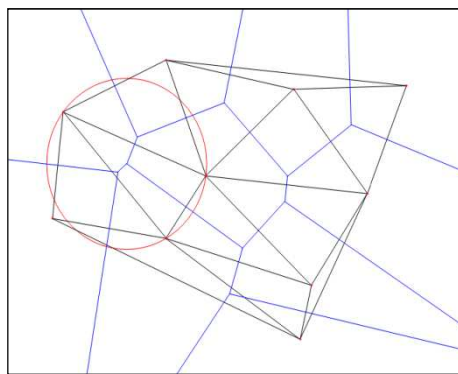


**Figure 1.** 2D point set (red dots), its Voronoi diagram (blue) and the Delaunay triangulation (black)

### 3. Expected mesh quality and algorithm requirements

The mesh of the dataset is a linear interpolation of the points, and is based on the Delaunay structure. The common approach for 3D datasets is to build a 3D Delaunay triangulation and extract triangular facets that are a linear approximation of the underlying surface. A good mesh quality is a mesh that approximates well the underlying surface and that connects the points correctly in accordance with the topology of the surface. The quality of the mesh sought is based on well-defined criteria. First, the reconstructed surface should be topologically equivalent to the underlying surface of the points set. This means that the reconstructed surface should be homeomorphic to a 2-manifold and to  $\mathbb{R}^2$ . In topology we usually refer to basic topological elements such as disks. A mesh is a discrete 2-manifold only if each vertex umbrella is homeomorphic to a 2-disk [13]. The umbrella of a point on a mesh is the set of triangles (and their vertices) that are incident to that point. Second, the reconstructed surface should also be geometrically equivalent to the underlying surface (figure 2). Both facet normals and surface normals should be similar in direction. Both representations should be geometrically close in terms of Hausdorff distance. The chord error between the facets and the surface should not exceed a given tolerance and be proportional to the sampling density. Surface reconstruction is the process of extracting the restricted Delaunay facets that approximate the first order of the surface out of the 3D Delaunay complex.

Algorithmic complexity is also a major issue to our application. The reconstruction algorithm is to be optimized with regard to space and time complexities. Space, because very large data need to be processed, and time because the characterization of the parts is an on-line process that should not exceed -at least- the measurement time. In fact, the Delaunay triangulation algorithm is incremental so it can be applied incrementally with a sequential insertion scheme as the points are being measured. Furthermore, in the case of an on-line metrology application, an automatic reconstruction process is required. No human intervention shall be necessary.

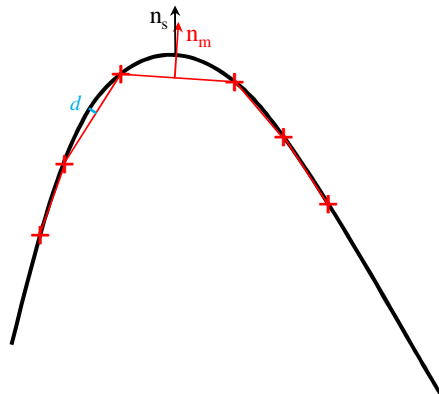


**Figure 2.** Geometrical equivalence between mesh and theoretical surface

## 4. Surface reconstruction

### 4.1 Alpha shapes

The Alpha shapes is a kick-off algorithm for surface reconstruction and is used as a data filter in applications such as in form fitting of freeform surfaces [5,11]. From the 3D Delaunay triangulation of the dataset, the  $\alpha$ -shape is an extracted sub-complex formed by all simplices that have the property of being  $\alpha$ -exposed. Figure 3 shows the difference between an  $\alpha$ -exposed simplex and a non  $\alpha$ -exposed simplex. The simplices considered are triangular facets. The algorithm passes a sphere of constant diameter  $\alpha$  across the facets and checks for its content. Either the sphere is empty of points and the facet is  $\alpha$ -exposed or the sphere contains points from the dataset and the facet is non  $\alpha$ -exposed. All the facets that are  $\alpha$ -exposed are selected and constitute the simplices of the output mesh. Alpha shapes are not designed to build manifold meshes but only an approximation of the shape inherent to the points. It can be shown that a non-uniform point distribution causes the result to be non manifold.

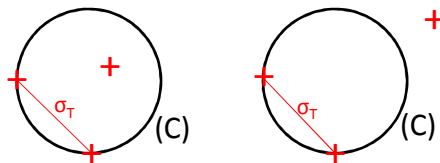


**Figure 3.** 2D example, a constant diameter circle. Non  $\alpha$ -exposed simplex (left),  $\alpha$ -exposed simplex (right)

### 4.2 Cocone

The Cocone algorithm was developed by Amenta *et al* for 2D curves and expanded to surfaces in 3D [3,6]. Cocone is the first algorithm to provide geometrical and topological guarantees which ensure the output triangular mesh is a good approximation of the surface to be reconstructed. These guarantees are conditioned by an  $\varepsilon$ -sampling condition on the dataset which is defined with respect to the local feature size at a given location on the surface. The condition states that any point  $x$  taken on the surface should have at least one sample point within the range of  $\varepsilon$  times the perpendicular distance from  $x$  to the medial axis of the surface. This perpendicular distance is called the local feature size of  $x$  and denoted  $LFS(x)$ . Therefore the  $\varepsilon$  condition requires that the medial axis of the surface exists and the surface is closed (2). Ultimately, it also implies that the sampling is denser in regions where the curvature is high, and inversely.

$$\|x - p\| \leq \varepsilon \cdot LFS(x), \quad \text{with } \varepsilon \leq 0,1 \quad (2)$$

The robustness of the Cocone algorithm highly depends on the  $\varepsilon$ -sampling condition. In the absence of it, the guarantees are dropped. The algorithm is based on the Delaunay triangulation and its dual representation, the Voronoi diagram of the point set. Once the Delaunay triangulation has been

constructed, the algorithm works on the triangular facets constituting the  $(n-1)$  simplices of the triangulation. The idea derives from the fact that the triangular facets of the output mesh are a first order approximation of the underlying surface. Each facet is thus an approximation of the tangent plane to the surface at the facet's location up to a chord error. It follows that the normal to the facet is an approximation of the surface normal at the same location. With this property, Cocone searches for the restricted Delaunay facets by stating that these are within a given tolerance zone delimited by a double cone. So if, within the conical zone, a facet should exist, it means that this facet belongs to the restricted Delaunay complex and that it is part of the output mesh.

The Cocone is defined by two geometrical elements and an angle: the axis, the apex and the opening angle. The cone axis is defined as being orthogonal to the approximate tangent plane. Let's assume that a facet  $f$  is a good approximation of the tangent plane to the surface at a certain location. The dual Voronoi element to a Delaunay facet is an edge that is orthogonal to the facet. Therefore, the dual Voronoi edge to  $f$  is in theory both, the approximation of the normal to the surface, and the axis of the Cocone of  $f$ . Since only some Voronoi edges are in the correct direction, the algorithm seeks those ones which are directionally close to the vector that connects a query point  $p$  to its pole. The poles of a Voronoi cell are the farthest two Voronoi vertices the cell. Amenta *et al* [6] have proven that these poles approximate the normal directions inwards and outwards at  $p$ . Consequently, for a given facet and its dual Voronoi edge, the Cocone test is applied. It consists of simulating the plot of a double cone at each vertex of the facet (figure 4). The normal approximation of a facet is approximated by its three vertices normals. If the Cocone condition is verified for all three vertices of a facet, the facet is selected in the output mesh.

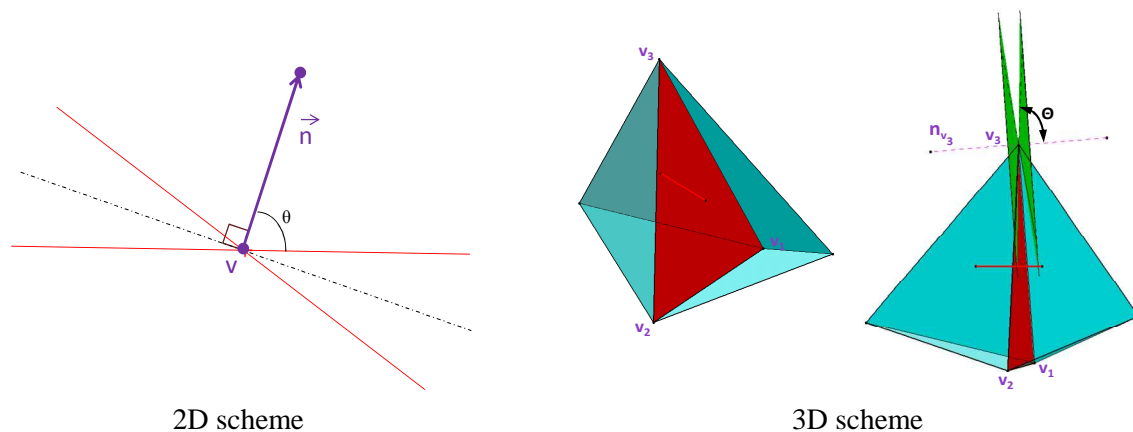


**Figure 4.** The Cocone condition at one vertex of the considered facet

#### 4.3 Other Methods

Other methods that were developed are also based on the  $\varepsilon$ -sampling condition. The Natural Neighbours Interpolation of Boissonnat and Cazals [14] follows, by some means, the same principle. It also seeks the restricted Delaunay facets and the dual Voronoi edges that approximate the normal direction. However, the detection of Voronoi edges is different. The algorithm calculates an implicit distance function on the points. This function would be the association of a scalar to a three dimensional point. The function returns a zero at the points of the dataset, a negative value inside the surface and a positive value outside. The Voronoi edges that have mixed vertex signs are edges that cross the implicit surface and are considered as a good approximation of surface normals. Figure 5 illustrates the logic behind this algorithm and shows Voronoi edges that are in the configuration sought and their dual restricted Delaunay elements.

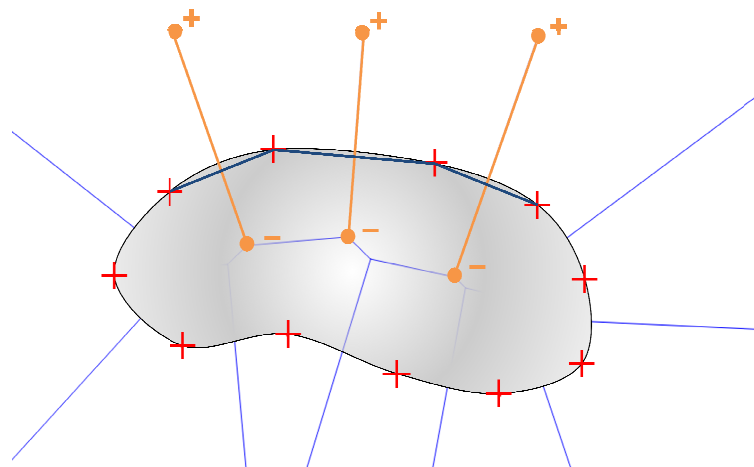


**Figure 5.** 2D example of the Natural Neighbours Interpolation algorithm

The Wrap algorithm of Edelsbrunner [15] follows a different approach to what preceded. It calculates a distance function on the points, identifies critical points through the gradient of that function and then builds a flow relation following the steepest ascent of the gradient. Grove [16] has previously shown that there exists a duality between critical points and the Delaunay and Voronoi simplices and their intersections. Based on this fact, flow relations congregate Delaunay simplices in clusters. Some clusters are stable manifolds and some others are unstable manifolds that need to be eliminated. The Wrap algorithm does not provide global guarantees, only locally at the stable manifold clusters level. The works of [17] and [18] have linked Wrap to the  $\epsilon$ -sampling theory and by that have demonstrated that Wrap can supply global topological and geometrical guarantees, again only if the  $\epsilon$ -sampling condition is satisfied.

Dey *et al* [19] continued working on the Cocone algorithm and developed what is known by enhanced Cocone algorithms. They discussed a version of the Cocone algorithm in which large datasets are processed via an Octree subdivision of the points space. Dey *et al* [20] proposes an algorithm with provable guarantees for noisy data. In theory, the noise is limited to a given limit proportional to that of the sampling. Practically, it performs poorer than the basic Cocone algorithm on the same non noisy dataset. The reason is that RobustCocone filters out tetrahedra associated to points that do not verify the noise level condition which is in turn very tight. The last publication on Cocone [21] puts forward a local approach to algorithmically reconstruct a surface from the 3D Delaunay triangulation. In fact, even the Delaunay triangulation is localized. Points are clustered into cells. The Delaunay triangulation is built piecewise, cell by cell, by considering the points of a cell and the points of a portion of the neighbouring cells.

Boissonnat and Ghosh proposed an algorithm based on tangential Delaunay complexes [22]. Instead of natural neighbours, tangential neighbours are computed and the approximation of Delaunay restricted simplices follows this kind of localized neighbourhood. The algorithm assumes the knowledge of normal directions and that the local feature size at any point is positively defined. So these additional constraining conditions make of this algorithm a specific one.

## 5. Comparison on a simple 2D point set

The sculpture algorithm as well as the alpha shapes and Cocone are compared in 2D. Matlab codes are generated on the same simple dataset showing the difference in algorithmic behaviour. Figure 6a shows a random dataset representing a curve in 2D and figure 6b shows the Delaunay triangulation of the set. The algorithms are all applied on the same dataset.



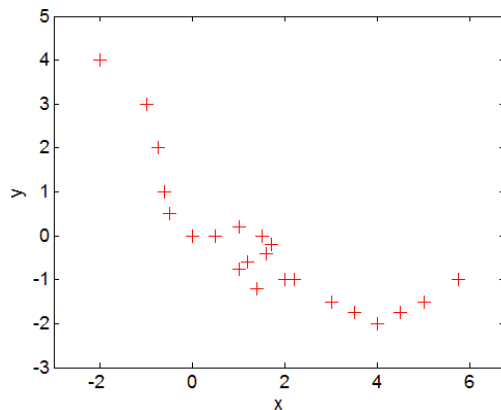


**Figure 6a.** 2D dataset of a curve

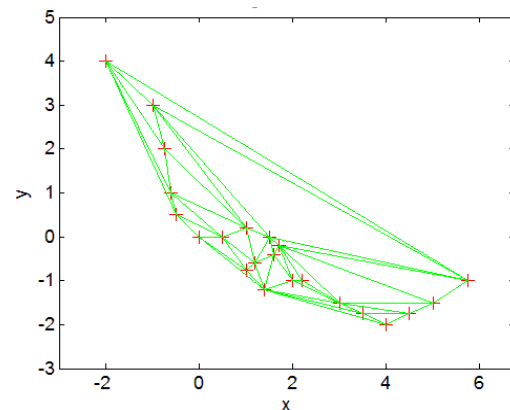


**Figure 6b.** Delaunay triangulation of the point set

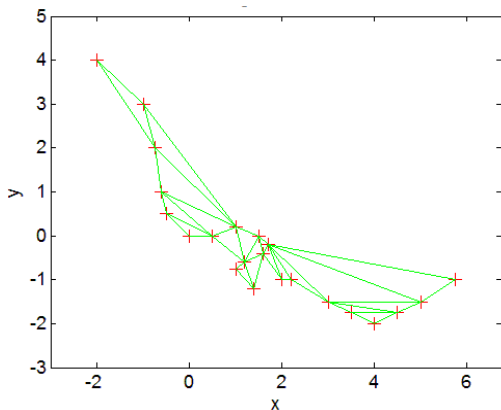


**Figure 6c.** Sculpture algorithm

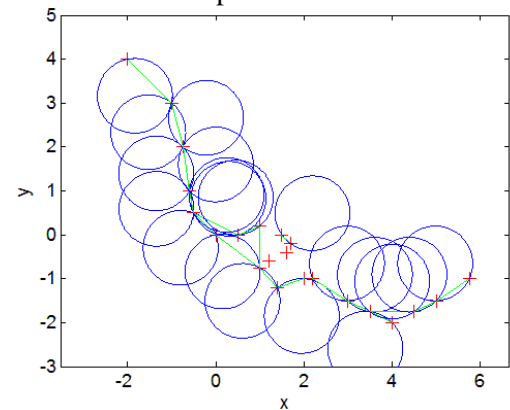


**Figure 6d.** Circles of constant diameter  $\alpha$  traversing Delaunay edges

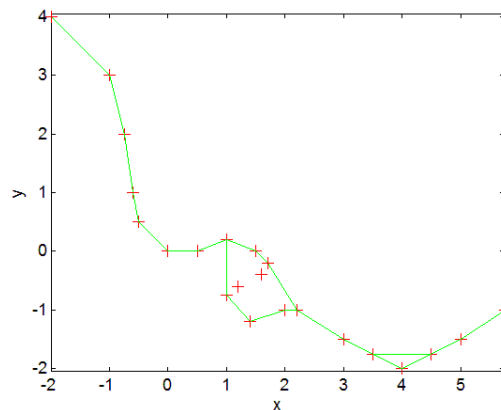


**Figure 6e.** Alpha shape

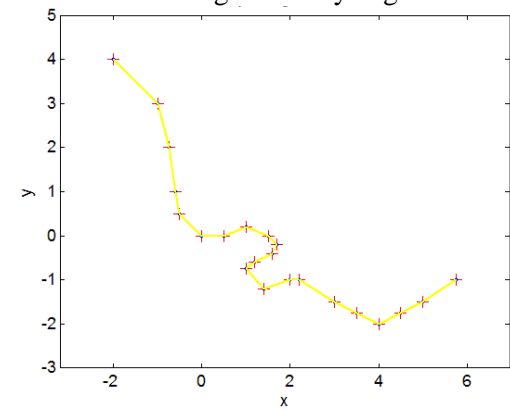


**Figure 6f.** Cocone

Figure 6c is the result of the sculpture algorithm of Boissonnat applied on the Delaunay triangles. By detecting interior points one after the other, associated triangles are sculpted out. Figure 6d shows the plot of circles of diameter  $\alpha=0.85$  tested at each segment. Delaunay edges are traversed because it is a 2D application. The circles that are empty of other points from the dataset and that cross a Delaunay edge are called  $\alpha$ -exposed edges. These edges constitute the  $\alpha$ -shape of the points shown in figure 6e. It is to notice how the  $\alpha$ -shape is not necessarily manifold. The Cocone result shown in figure 6f is manifold. Cocone reconstructs the curve only because it respects the  $\varepsilon$ -sampling condition. In the central region where the curvature is high a high point density is required, unlike low curvature regions.

Based on the above comparison, the comparison in table 1 and the abundance of the Cocone citations in literature, the Cocone algorithm best fits our application. Guarantees and algorithmic complexity are the two major criteria on which the comparison is made. Another decisive criterion is the possibility to process large data. The Wrap algorithm requires that a flow relation is calculated over the Delaunay simplices and this is a relationship-based computation. Simplices cannot be treated independently. So provided that the number of Delaunay simplices is very large, the algorithm comes to a crash for excessive memory load. Unlike Wrap, the Natural Neighbours Interpolation algorithm calculates a distance function over the points and then treats the Voronoi edges separately. However, this algorithm works only on closed surfaces since it requires the knowledge of inside and outside spaces with respect to the surface. With Cocone algorithm, each facet and its dual Voronoi edge undergo the Cocone test one by one which gives it the advantage of hashing and parallelization. In addition, it does not need any information regarding inside and outside spaces. The only input, which can be generalized to an acceptable value, is the angle  $\Theta$  of the Cocone.

Table 1: Comparison of surface reconstruction algorithms

	<b>Complexity</b>	<b>Guarantees</b>	<b>Large datasets</b>	<b>Sampling</b>	<b>Input information</b>
Sculpture	$N^2 \cdot \log N$	x	x	x	x
$\alpha$ -shapes	$N^2$	x	x	x	x
Cocone	$N^2$	✓	x	$\varepsilon \leq 0.05$	$\Theta$
N.N.Interp	$N^2$	✓	✓	$\varepsilon \leq 0.25$	Inside & outside spaces
Wrap	$N^2$	✓	x	$\varepsilon \leq 0.01$	x
Convection	$N^2$ (local)	x	✓	x	Normal direction
Tangential complexes	$N^2$ (local)	✓	✓	$\varepsilon \leq 0.09$	Normals
LocCocone	$N^2$ (local)	✓	✓	$\varepsilon \leq 0.05$	$\Theta$

## 6. Example of application of the Cocone method to measured optical lens surfaces

The idea here is to investigate surface reconstruction methods and to apply an algorithm that would build a data structure on the initially unstructured 3D point sets and that would transform the discrete point clouds into continuous piecewise linear representations. For applications such as profile metrology, it is crucial to have a continuous representation. Profile metrology is an application where dimensional characteristics are estimated on an extracted cross section of the surface. Yet, another application to surface reconstruction relates to ray-tracing simulation of optical parts. An this application requires to have a mesh representation [23].

To be representative of most common applications in 3D metrology of complex optical surfaces, an optical lens measured in two different strategies is considered. The optical lens is an asphere defined by the analytical equation (3).

The first set of measured points on an XY grid basis contains 2,782,224 points over a squared area of 5x5mm. The measurement is done using the reference profilometer developed at LNE. It ensures three degrees of freedom, x, y and z linear motions and perfectly respects the Abbe



principle. Its metrology loop is optimized to be as short as possible. The part only moves in the XY-plane and the probe moves only along the z axis. The second set of points contains more than 1,000,000 points covering the entire surface and is measured using the Nanomefos machine. The part is mounted on a rotating table. An optical sensor is focused at the centre of the part and while the latter undergoes rotation, the measuring head moves in the radial direction from the centre outwards.

$$Z(r) = \frac{\frac{r^2}{R}}{1 + \sqrt{1 - \frac{r^2}{R^2(1+\kappa)}}} + \sum_{n=1}^m \alpha_{2n} \cdot r^{2n} \quad (3)$$

The Cocone algorithm was implemented and tested on both datasets. These datasets are known to be excessively dense. Figures 7 and 8 (left) show the failure of this algorithm for the fact that the  $\varepsilon$ -sampling condition is not fulfilled on the datasets. Figures 7 and 8 (right) show that when the sampling respects the  $\varepsilon$  condition, the reconstruction is proper. The reconstruction algorithms cited in the previous section are very sensitive to the  $\varepsilon$ -sampling condition. The implementation of the Cocone algorithm has put into evidence the limitation related to having overly dense sampled data.

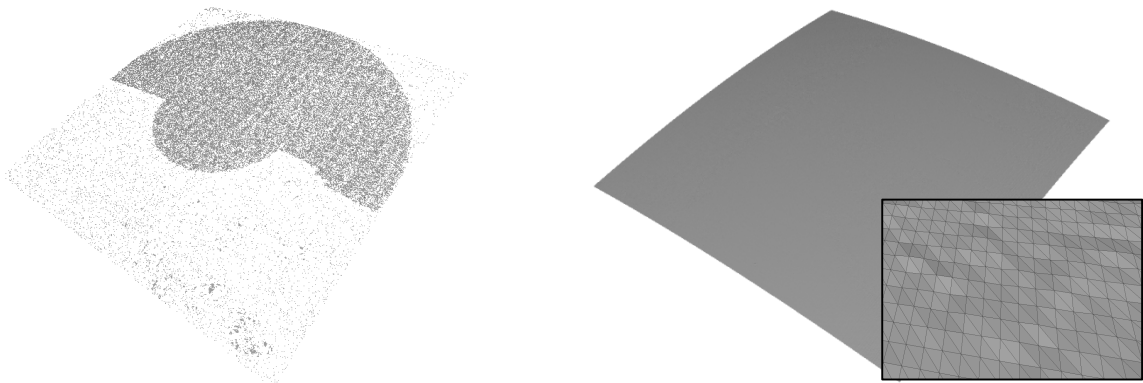


**Figure 7.** Optical lens reconstruction from measurement made by LNE (XY grid): Original dataset not respecting  $\varepsilon$ -sampling (left, 2,782,224 points), filtered dataset respecting  $\varepsilon$ -sampling (right, 1,023,300 points)

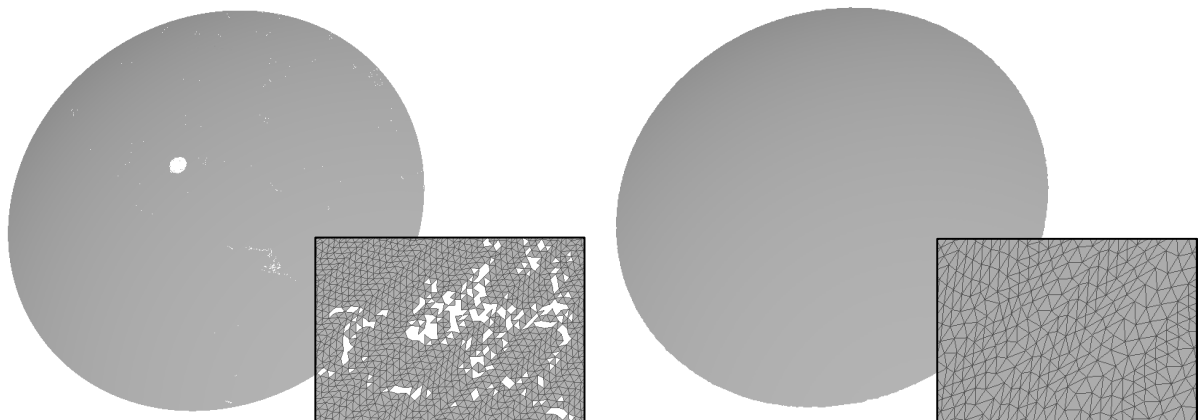


**Figure 8.** Optical lens reconstruction from measurement made by TNO (spiral scan): Original dataset not respecting  $\varepsilon$ -sampling (left, 1,044,336 points), filtered dataset respecting  $\varepsilon$ -sampling (right, 301,698 points)

Optical surfaces, whether they have aspheric or freeform shapes, are usually almost flat surfaces. Irrespective of the measurement strategy, the resulting cloud of points is a set of points that can be projected onto a plane following a bijective mapping without any superposition of points from different sides of the surface. Non bijective projections result from freeform surfaces that represent superposition of points once projected onto a plane. An example of such surfaces is turbine blades. The bijection property offers the advantage of tracing back the points to their original position without modifying either the geometry or the topology of the underlying surface. Since topology is preserved on the map, neighbourhood is conserved and points can thus be meshed in a 2D-like fashion. The application of a 2D Delaunay triangulation is the best solution as it ensures the most regular and complete triangulation possible. The data structure is built in 2D and then mapped back to 3D as simplified in figure 9. The links created among the points are preserved. Figures 10 and 11 show the resulting triangulation based on this technique on both datasets without any filtering or modification of the points. The reconstruction is proper.

With the data structure created on the points, the association of the dataset to the theoretical model of aspherical surfaces is improved. Normal and curvature estimations are more precise since they are calculated based on the true neighbourhood of a point which is the neighbourhood found on the manifold and not in the 3D neighbourhood of the point [24].

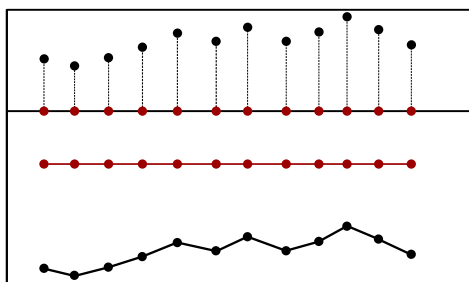


**Figure 9.** Top to bottom: projectable 3D point set, 2D Delaunay triangulation and inverse mapping

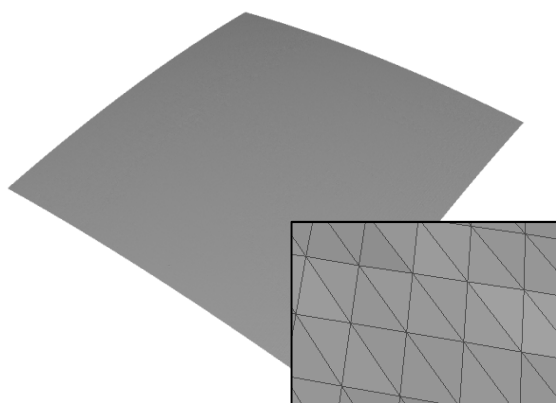


**Figure 10.** Optical lens reconstruction from original dataset measured by LNE (XY grid)

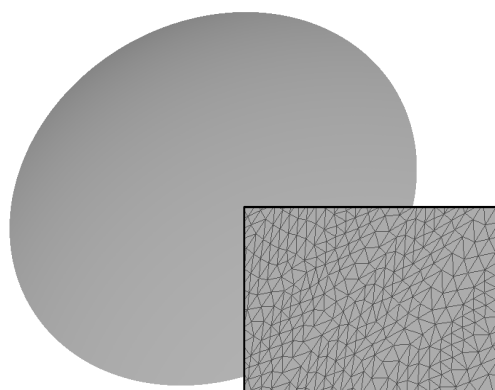


**Figure 11.** Optical lens reconstruction from original dataset measured by TNO (spiral scan)

## 7. Conclusion

In this paper, a comparison of surface reconstruction algorithms is presented and lead to the choice of Cocone which fits at best our application. The chosen algorithm possesses inherent limitations related to sampling density. The tests run on real measured optical lenses highlighted the necessity of having an  $\varepsilon$ -sampled point set. If the cloud of points does not respect the  $\varepsilon$  condition, a filter is required in order to reduce the overly dense dataset. With surface reconstruction, the underlying surface can be approximated by a first order representation called the mesh. The mesh builds a data structure for

initially unstructured points and most importantly creates a continuous representation of the surface. This is required whenever profile extraction and dimensional metrology are to be applied at some specified location on the surface. The mesh also offers the possibility to perform partition of the mesh vertices and thus the possibility to either apply reverse engineering or geometric feature extraction. However, the mesh is used here to structure data and to create a continuous representation of the underlying surface. A mesh is a more substantial structure to approximate normals and curvatures. Curvature estimation is an important tool for surface defects detection and for filtration which can be applied on the mesh vertices in order to reduce their number. Consequently, fitting becomes less complex. A future extension of this work will cover freeform surfaces such as freeform optics or turbine blades.

## 8. Acknowledgment

1-The authors sincerely thank the EMRP organization. The EMRP is jointly funded by the EMRP participating countries within EURAMET and the European Union (IND10).

2-The authors also thank TNO for the experimental dataset provided, especially Dr. Rens Henselmans.

## 9. References

- [1] Cazals F and Giesen J 2004 Delaunay triangulation based surface reconstruction: ideas and algorithms *In Effective Computational Geometry for Curves and Surfaces, J Boissonnat and M Teillaud (Eds.)* Springer-Verlag (2006) pp 231–276
- [2] Osher S and Fedkiw R 2002 *Level Set Methods and Dynamic Implicit Surfaces*. Applied Mathematical Sciences **153** (New York: Springer-Verlag)
- [3] Amenta N, Bern M and Eppstein D 1997 The crust and  $\beta$ -skeleton : combinatorial curve reconstruction *Graph. Mod. and Im. Proc.* **60** 125-135
- [4] Boissonnat J-D 1984 Geometric structures for three-dimensional shape representation *ACM Trans. on Graph.* **3** No.4 266-286
- [5] Edelsbrunner H and Mücke E 1994 Three dimensional alpha shapes *ACM Trans. on Graph.* **13** 43-72
- [6] Amenta N, Choi S, Dey T and Leekha N 2000 A Simple Algorithm for homeomorphic surface reconstruction. *Internat. J. Comput. Geom. Appl.* **12** 125-141
- [7] Savio E, De Chiffre L and Schmitt R 2007 Metrology of freeform shaped parts *CIRP Annals-Manuf. Tech.* **56** (2) 810-835 Elsevier
- [8] ISO/TS 17450-1:2005 Geometrical product specifications (GPS) - General concepts - Part 1: Model for geometrical specification and verification
- [9] Klocke F and Dambon O 2003 Precision machining of glass for optical applications *Proc. Of Int. Work. on Extr. Opt. and Sens. Tokyo, Japan* 185-193
- [10] Jiang X, Scott P, Whitehouse D and Blunt L 2007 Paradigm shifts in surface metrology part II the current shift *Proc. R. Soc. A* **463** 2071-99
- [11] Zhang X, Jiang X and Scott P 2011 A minimax fitting algorithm for ultra-precision aspheric surfaces. *Proc. 13th Intern. Conf. on Met. and Prop. of Eng. Surf.* 285-289, *National Physical Laboratory, Teddington, UK*
- [12] ISO 10110-12:2007 Optics and photonics -- preparation of drawings for optical elements and systems -- part 12: aspheric surfaces
- [13] Dyer R, Zhang H and Möller T 2009 A survey of Delaunay structures for surface representation *Tech. Rep. 2009-01, GrUVi Lab, School of Computing Science*
- [14] Boissonnat J-D and Cazals F 2000 Smooth surface reconstruction via Natural Neighbour interpolation of distance functions *Proc. 16th Ann. Symp. Comput. Geom.* 2000, 223-232
- [15] Edelsbrunner H 2003 Surface reconstruction by wrapping finite sets in space *Disc. & Comput. Geom.* **32** (2004) 231–244

- [16] Grove K 1993 Critical Point Theory for Distance Functions *Proc. of Symp. In Pure Math.* **54** (3) 357-385
- [17] Dey T, Giesen J, Ramos E and Sadri B 2005 Critical points of the distance to an epsilon-sampling of a surface and flow-complex-based surface reconstruction *Proc. of the 21st Ann. Symp. on Comput. Geom.* 218-227
- [18] Ramos E and Sadri B 2007 Geometric and topological guarantees for the Wrap reconstruction algorithm *Proc. of the 18th Ann. ACM-SIAM Symp. on Discr. Algo.*
- [19] Dey T, Giesen J and Hudson J 2001 Delaunay based shape reconstruction from large data *Proc. IEEE Symp. in Paral. and Large Data Visual. and Graph.* 19-27
- [20] Dey T and Goswami S 2004 Provable surface reconstruction from noisy samples *In Comput. Geom.: Theory & Appl.* **62**
- [21] Dey T, Dyer R and Wang L 2011 Localized cocone surface reconstruction *In Computers & Graphics* **35** 483-491
- [22] Boissonnat J-D and Ghosh A 2009 Manifold reconstruction using tangential Delaunay complexes *Proc. of ACM symp. on Comput. Geom.* 324-333
- [23] Morita S *et al* 2010 Ray-tracing simulation method using piecewise quadratic interpolant for aspheric optical systems *Appl. Opt.* **49** 3442-51
- [24] Smith T and Farouki R 2001 Gauss map computation for free-form surfaces *Comp. Aid. Geom. Des.* **18** 831-850